

# Optimizing Sensory Neurons: Nonlinear Attention Mechanisms for Accelerated Convergence in Permutation-Invariant Neural Networks for Reinforcement Learning

Junaid Muzaffar<sup>1\*</sup>, Khubaib Ahmed<sup>1</sup>, Ingo Frommholz<sup>2</sup>, Zeeshan Pervez<sup>1</sup>, Ahsan ul Haq<sup>3</sup>

## Abstract

*Training reinforcement learning (RL) agents often requires significant computational resources and extended training times. To address this, we build upon the foundation laid by [1] which introduced a novel neural architecture for reinforcement learning tasks that maintained permutation invariance in the sensory neuron system. While the baseline model demonstrated significant performance improvements over traditional approaches, we identified opportunities to enhance the efficiency of the learning process further. We propose a modified attention mechanism incorporating a non-linear transformation of the key vectors ( $K$ ) using a mapping function, resulting in a new set of key vectors ( $K'$ ). This non-linear mapping enhances the representational capacity of the attention mechanism, allowing the model to encode more complex feature interactions and accelerating convergence without compromising performance. Our enhanced model demonstrates significant improvements in learning efficiency, showcasing the potential for non-linear attention mechanisms in advancing reinforcement learning algorithms.*

## 1. Introduction

Modern deep learning systems typically struggle when faced with a sudden reordering of sensory inputs. This limitation often necessitates either model retraining or manual correction of the input order, posing significant challenges in dynamic environments. Techniques from continual meta-learning, such as adaptive weights [2–4], Hebbian learning [5–7], and model-based approaches [8–11], offer some potential in enabling models to adapt to such changes, but they often fall short when sensory input order varies unpredictably. In reinforcement learning (RL), where agents must navigate complex environments, the ability to process sensory inputs in a permutation-invariant manner is crucial for achieving robustness and generalization.

To address this problem, the concept of treating each sensory input as an independent neuron, as proposed in [1] offers a promising solution. In this approach, each sensory input is processed by an individual neural network module that integrates information from its specific sensory channel over time while also broadcasting its output message to other modules. Inspired by the Set Transformer architecture [12, 13], these messages are then combined via an attention mechanism to form a global latent representation, which is used to determine the agent’s actions. This system can handle an arbitrary number of sensory inputs processed in any random order, allowing the agent to maintain a coherent policy even when the input order is shuffled multiple times during an episode. This method not only makes the system robust to input permutations but also enables it to generalize better to new, unseen situations, such as environments with novel visual backgrounds or additional noisy input channels.

However, the computational and energy resources required to train such models are significant, especially when considering the complexity of self-attention mechanisms in handling a large number of sensory inputs. These requirements pose a considerable challenge in deploying these systems at scale. We address this as an optimization problem and propose an enhanced version of the sensory neuron that incorporates a nonlinear attention mechanism. This modification not only reduces the computational overhead but also accelerates the convergence of the learning process. We introduced a nonlinear mapping function, which is applied before the attention mechanism, resulting in a more expressive feature representation and improved gradient dynamics. Through extensive experimentation in various RL environments, we demonstrate that our approach leads to faster convergence and better generalization, providing a practical and efficient solution for permutation-invariant reinforcement learning.

Our model offers several key advantages over traditional approaches in permutation-invariant reinforcement learning. First, by incorporating a nonlinear attention mechanism, our model significantly enhances the expressiveness of the fea-

<sup>1</sup>Faculty of Science and Engineering, University of Wolverhampton, Wolverhampton, UK. <sup>2</sup>School of Applied Data Science, Modul University, Vienna, Austria. <sup>3</sup>Department of Mathematics, University of Technology Applied Sciences, Suhar, Oman

ture space, allowing for more nuanced and effective policy decisions. This increased expressiveness translates into faster convergence rates, enabling the model to learn optimal policies more quickly, even in complex environments. Additionally, the model’s robustness to random reordering of sensory inputs ensures that it can maintain consistent performance across varying scenarios, including those with noisy or redundant information. The computational efficiency gained through our optimized attention mechanism also reduces the resource demands typically associated with training such models, making it more feasible to deploy in real-world applications. Furthermore, our approach generalizes well to unseen environments, demonstrating adaptability to new visual features and input variations without the need for retraining, thus providing a more scalable and versatile solution for reinforcement learning tasks.

## 2. Related Work

**Attention mechanisms** serve as dynamic weighting systems that adjust neural network connections based on input characteristics. The concept of linear dot-product attention was initially introduced in the context of meta-learning [14], with subsequent versions incorporating softmax non-linearity emerging later [15, 16]. This mechanism gained widespread recognition through its implementation in the Transformer model [13], which greatly enhanced its expressive capabilities, allowing it to derive inductive biases from extensive datasets. Such capabilities have led to the integration of attention mechanisms into leading-edge applications across various fields, including natural language processing [17, 18], image recognition and generation [19, 20], and multimedia processing [21–23]. In the realm of reinforcement learning (RL), attention mechanisms have been effectively utilized [24–28], particularly in our study, which leverages these mechanisms to facilitate inter-module communication within an RL agent.

**Set Transformers** [12] were designed to efficiently manage set-structured data through a permutation-invariant approach using self-attention mechanisms, adapted from the widely utilized Transformer [13] model in natural language processing. This architecture excels in processing sets—unordered collections of elements—making it ideal for applications where input data does not adhere to a sequential format. The self-attention in the Set Transformer allows for comprehensive interaction analysis between all elements in a set, ensuring consistent output regardless of the input order. This capability is vital for tasks such as point cloud processing and feature set analysis, where the data’s order can vary but should not impact the analysis outcome, thereby enhancing the flexibility and utility of attention mechanisms in broader, more generalized settings.

**Sensory Neuron** [1] explores the application of sensory neurons modeled as transformers to achieve permutation

invariance in neural networks designed for reinforcement learning tasks. This approach conceptualizes each sensory input as an independent neuron within a transformer architecture, enabling the model to handle arbitrary reordering of inputs without loss of performance. By using an attention mechanism, the model dynamically adjusts to changes in input order, ensuring that the system remains invariant to permutations of the sensory data. This design not only enhances the flexibility and adaptability of the neural network in dealing with varied and dynamic environments but also improves its ability to generalize across different situational contexts, making it particularly effective for reinforcement learning applications where input order can frequently change. This foundational work laid the groundwork for our research, enabling us to further optimize the model for faster convergence and achieve early and effective convergence in our applications.

## 3. Method

### 3.1 Background

To achieve permutation invariance within sensory inputs for reinforcement learning agents, [1] introduced a novel attention-based neural architecture that processes arbitrarily ordered sensory inputs without requiring retraining for input permutations. Letting  $o_t$  denote the agent’s current observation (comprising multiple sensory inputs), each observation component  $o_t[i]$  is fed into an independent sensory neuron, a neural network module that processes the input locally. These sensory neurons, acting independently, compute key-value message pairs  $f_k(o_t[i], a_{t-1})$  and  $f_v(o_t[i])$ , where  $a_{t-1}$  denotes the previous action. These messages are then aggregated by an attention mechanism to form a global latent code  $m_t$ , which serves as the input to the agent’s policy network, enabling the agent to derive a coherent policy across randomly ordered inputs.

The permutation invariance of the model is achieved through the attention mechanism’s self-attention operation, expressed as:

$$m_t = \sigma \left( \frac{[QW_q][K(o_t, a_{t-1})W_k]^\top}{\sqrt{d_q}} \right) [V(o_t)W_v] \quad (1)$$

where  $Q$  is a matrix of fixed embeddings [29], and  $K(o_t, a_{t-1})$  and  $V(o_t)$  represent key and value matrices derived from the sensory neurons’ outputs. The function  $\sigma$  is a non-linear activation function (e.g., softmax) that ensures the attention weights adapt based on the input configuration. Since permuting the sensory input order only alters the row ordering of  $K$  and  $V$ , but not the resulting output  $m_t$ , the global latent code remains invariant to any permutation of the input indices. This architecture, therefore, enables agents to retain robust, task-relevant represen-

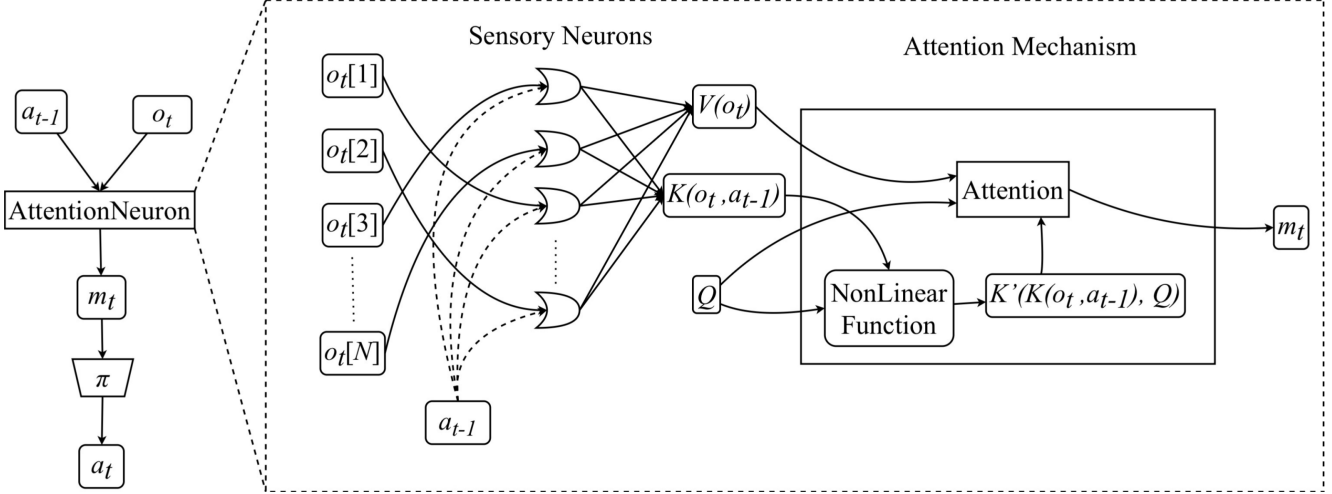


Figure 1: *Overview of Nonlinear Attention Mechanism.* The AttentionNeuron layer independently processes each sensory input  $o_t[i]$  along with the previous action  $a_{t-1}$  to handle unordered observations. Each sensory neuron computes  $V(o_t)$  and  $K(o_t, a_{t-1})$ , representing value and key functions respectively. A nonlinear function then maps  $K(o_t, a_{t-1})$  and the fixed vector  $Q$  to generate  $K'(K(o_t, a_{t-1}), Q)$ . The attention mechanism subsequently uses these transformed keys and values to create a global latent message  $m_t$ .

tations across changing input orders, yielding policies that generalize effectively to dynamic and unordered input configurations without retraining. Our aim is to optimize the attention mechanism in such a way that it improves convergence time of the agent without compromising agent’s performance, and we do that with our nonlinear attention mechanism.

### 3.2 Nonlinear Attention Mechanism

To develop permutation-invariant (PI) agents, [1] proposed adding an additional layer before the agent’s policy network  $\pi$ . This layer takes the current observation  $o_t$  and the previous action  $a_{t-1}$  as inputs. They refer to this new layer as the AttentionNeuron. To optimize this AttentionNeuron layer, we introduce the nonlinear attention mechanism, where we propose a nonlinear function, Figure 1 shows the overview of the proposed nonlinear attention mechanism.

The following equations explain the overall operations inside the modified AttentionNeuron, and for clarity Table 1 lists the notations used in these equations.

$$K(o_t, a_{t-1}) = \begin{bmatrix} f_k(o_t[1], a_{t-1}) \\ \vdots \\ f_k(o_t[N], a_{t-1}) \end{bmatrix} \in \mathbb{R}^{N \times d_{f_k}}, \quad (2)$$

$$V(o_t) = \begin{bmatrix} f_v(o_t[1]) \\ \vdots \\ f_v(o_t[N]) \end{bmatrix} \in \mathbb{R}^{N \times d_{f_v}}$$

$$K' = K^2 + 2K + Q|1 + K| \quad (3)$$

$$m_t = \sigma \left( \frac{[QW_q][K'(K(o_t, a_{t-1}), Q)W'_k]^\top}{\sqrt{d_q}} \right) [V(o_t)W_v] \quad (4)$$

Equation 2 illustrates how each of the  $N$  sensory neurons independently generates its messages,  $f_k$  and  $f_v$ , which are shared functions applied across all sensory neurons. Equation 3 is used to introduce nonlinearity and a piecewise linear component that significantly enhance gradient flow. The transformed vector  $K'$  possesses a richer representation due to the application of the nonlinear mapping. The quadratic term  $K^2$  enables  $K'$  to capture intricate relationships between input features, while the piecewise linear component provides a mechanism akin to attention, particularly accentuating regions where  $K$  approaches  $-1$ . Furthermore, the fixed  $Q$  vector provides stability in this transformation, maintaining consistency across different permutations, which is crucial for learning in permutation-invariant tasks. This dual contribution results in a more expressive feature space, enhancing the ability to differentiate between various states or actions, thereby supporting more effective policy learning.

Incorporating  $K'$  within the self-attention mechanism allows the attention weights to reflect this enriched representation, enabling the model to emphasize the most relevant aspects of the input space. Such selective focus is especially pivotal in reinforcement learning, where accurately identifying and leveraging key environmental features can

Table 1: Summary of notation and dimensionalities used across different RL environments in our experiments.

Description	Notation	CartPole	Ant	CarRacing	Atari Pong
Full observation space	$o_t$	$\mathbb{R}^5$	$\mathbb{R}^{28}$	$\mathbb{R}^{96 \times 96 \times 4}$	$\mathbb{R}^{84 \times 84 \times 4}$
Individual sensory input	$o_t[i]$	$\mathbb{R}^1$	$\mathbb{R}^1$	$6 \times 6 \times 4 = 144$	$6 \times 6 \times 4 = 144$
Number of sensory neurons	$N$	5	28	$(96/6)^2 = 256$	$(84/6)^2 = 196$
Dimension of action space	$ \mathcal{A} $	1	8	3	6 (one-hot)
Number of embeddings in $Q$	$(M)$	16	32	1024	400
Projection matrix for $Q$	$(W_q)$	$\mathbb{R}^{8 \times 32}$	$\mathbb{R}^{8 \times 32}$	$\mathbb{R}^{8 \times 16}$	$\mathbb{R}^{8 \times 32}$
Projection matrix for $K$	$(W_k)$	$\mathbb{R}^{8 \times 32}$	$\mathbb{R}^{8 \times 32}$	$\mathbb{R}^{111 \times 16}$	$\mathbb{R}^{114 \times 32}$
Projection matrix for $V$	$(W_v)$	$I$	$I$	$\mathbb{R}^{144 \times 16}$	$\mathbb{R}^{144 \times 32}$
Post-attention activation	$\sigma(\cdot)$	tanh	tanh	softmax	softmax
Global latent code	$m_t$	$\mathbb{R}^{16}$	$\mathbb{R}^{32}$	$\mathbb{R}^{1024 \times 16}$	$\mathbb{R}^{400 \times 32}$

Note: The projection matrix for the transformed key vector  $K'$  has the same dimensionality as  $K$ .

significantly expedite the learning process and improve the overall performance of the agent.

Moreover, equation 4 captures the transformation of sensory inputs into a robust latent code  $m_t$ , utilizing both non-linear and attention mechanisms to enhance feature representation. By integrating the non-linear mapping  $K'$  within the self-attention mechanism, the model generates attention weights that emphasize critical elements of the input space. This selective focus, driven by  $K'$ 's enriched feature space, enables the model to distinguish between subtle environmental variations, crucial for accurate policy learning.

In reinforcement learning, where identifying and leveraging key features can accelerate the learning process, this attention-enhanced representation is especially valuable. Through the consistent influence of the fixed vector  $Q$ , the transformation stabilizes across permutations, supporting the model's ability to learn invariant representations without compromising adaptability. Consequently, the resulting latent code  $m_t$  not only reflects a rich, permutation-invariant summary of the observation  $o_t$  but also empowers the agent to prioritize information effectively, leading to more precise and efficient decision making.

To formalize the model's operation, Algorithm 1 details the computation from observation to action using the proposed NLA mechanism.

#### 4. Experiments

To evaluate the effectiveness of our non-linear attention mechanism in PI-RL agents, we conduct experiments on RL environments similar to [1]. Given the distinct nature of these tasks, we describe the different policy network architectures and training methodologies employed. However, since all agents share the same fundamental AttentionNeuron structure (with nonlinear attention), we first outline the common setup.

---

#### Algorithm 1: Forward Pass with Nonlinear Attention (NLA)

---

**Input:** Observation  $o_t$ , previous action  $a_{t-1}$ , query set  $Q$ , shared functions  $f_k, f_v$ , projection matrices  $W_q, W_k, W'_k, W_v$

**Output:** Action  $a_t$

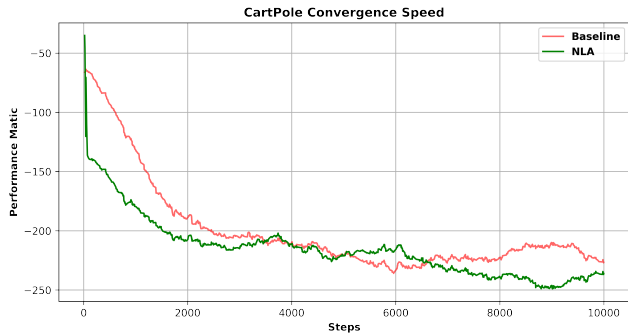
```

/* Let  $d_k$  be the dimensionality of
   key/query vectors, and  $d_v$  of
   value vectors */
1 Split  $o_t$  into  $N$  sensory elements:  $[o_t[1], \dots, o_t[N]]$ ;
2 for  $i = 1$  to  $N$  do
3    $k_i \leftarrow f_k(o_t[i], a_{t-1})$ ; // Compute key
   from sensory input
4    $v_i \leftarrow f_v(o_t[i])$ ; // Compute value from
   sensory input
5  $K \leftarrow [k_1, \dots, k_N] \in \mathbb{R}^{N \times d_k}$ ;
6  $V \leftarrow [v_1, \dots, v_N] \in \mathbb{R}^{N \times d_v}$ ;
7  $Q_{\text{proj}} \leftarrow Q \cdot W_q \in \mathbb{R}^{M \times d_k}$ ;
8  $K_{\text{proj}} \leftarrow K \cdot W_k \in \mathbb{R}^{N \times d_k}$ ;
   // Apply Nonlinear Attention
   transformation to keys
9  $K' \leftarrow K_{\text{proj}}^2 + 2K_{\text{proj}} + Q_{\text{proj}} \cdot |1 + K_{\text{proj}}|$ ;
10  $V_{\text{proj}} \leftarrow V \cdot W_v \in \mathbb{R}^{N \times d_v}$ ;
11 AttentionWeights  $\leftarrow \text{softmax}\left(\frac{Q_{\text{proj}} \cdot K'^T}{\sqrt{d_k}}\right)$ ;
12  $m_t \leftarrow \sigma(\text{AttentionWeights} \cdot V_{\text{proj}})$ ; // Latent
   representation
13  $a_t \leftarrow \text{PolicyNetwork}(m_t)$ ; // Output action

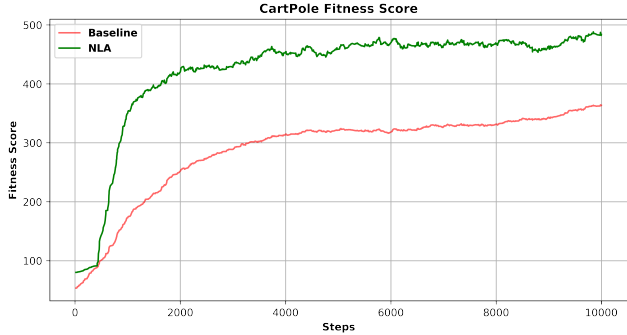
```

---

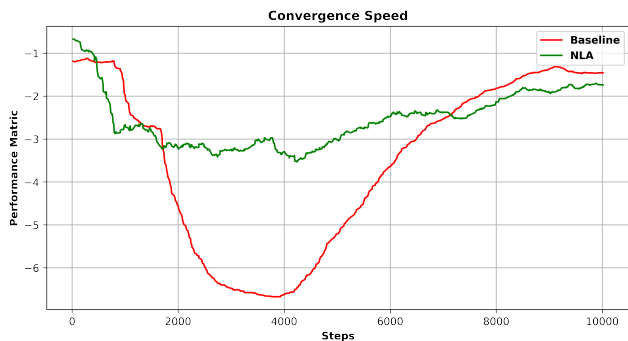
For tasks involving non-visual continuous control, the agent receives an observation vector  $o_t \in \mathbb{R}^{|O|}$  at each timestep  $t$ . We assign  $N = |O|$  sensory neurons, with each neuron processing a single element from the observation vector, i.e.,



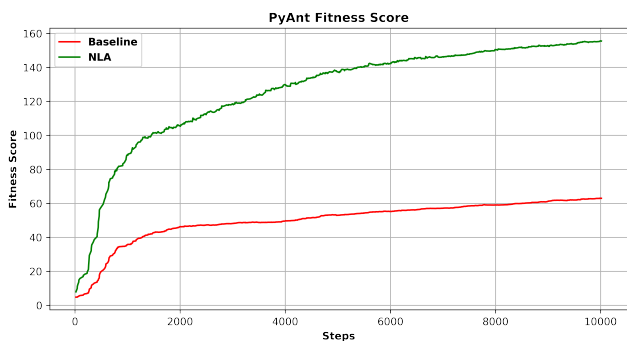
(a) CartPole Convergence Speed



(b) CartPole Max Fitness Score



(c) PyBullet Ant Convergence Speed



(d) PyBullet Ant Max Fitness Score

Figure 2: Comparison of convergence speed and max fitness score for CartPole Swing-Up and PyBullet Ant tasks. The first row (a, b) shows results for the CartPole task, where the NLA model exhibits faster convergence (a) and reaches a higher fitness score earlier (b) compared to the baseline. The second row (c, d) presents results for the PyBullet Ant task, where the NLA model also demonstrates more stable learning dynamics (c) and superior final performance (d).

$o_t[i] \in \mathbb{R}^1$  for  $i = 1, \dots, |O|$ . To generate the Keys, we use an LSTM [30] for  $f_k(o_t[i], a_{t-1})$ , with an input size of  $1 + |A|$  (2 for Cart-Pole and 9 for PyBullet Ant). The function  $f_v(o_t[i])$  is a simple identity mapping  $f(x) = x$ , which ensures that  $V(o_t)$  directly represents the processed inputs. The activation function  $\sigma(\cdot)$  is set to  $\tanh$ . We follow the baseline approach by setting  $W_v = I$ , so the learnable parameters in this set-up include the LSTM,  $W_q$ , and  $W_k$ .

For vision-based tasks, we preprocess observations by converting them to grayscale and stacking  $k = 4$  consecutive RGB frames from the environment. Thus, the agent receives  $o_t \in \mathbb{R}^{H \times W \times k}$ . Each observation is partitioned into non-overlapping patches of size  $P = 6$  using a sliding window, so each sensory neuron observes  $o_t[i] \in \mathbb{R}^{6 \times 6 \times k}$ . The function  $f_v(o_t[i])$  flattens the input, producing  $V(o_t)$  as a tensor of shape  $N \times d_{f_v} = N \times (6 \times 6 \times 4) = N \times 144$ .

Given the high-dimensional nature of visual tasks, we replace recurrent models with a more straightforward approach to process sensory inputs. The function  $f_k(o_t[i], a_{t-1})$  computes the difference between consecutive frames, flattens the result, appends  $a_{t-1}$ , and returns

the concatenated vector. Consequently,  $K(o_t, a_{t-1})$  forms a tensor of shape  $N \times d_{f_k} = N \times [(6 \times 6 \times 3) + |A|] = N \times (108 + |A|)$ , yielding dimensions of  $N \times 111$  for Car-Racing and  $N \times 114$  for Atari Pong. We use the softmax function as the activation  $\sigma(\cdot)$  and apply layer normalization [31] to both input patches and the resulting latent code.

#### 4.1 Cart-pole Swing Up

The CartPole Swing-Up [32–34] task is a standard reinforcement learning benchmark for studying control policies and attention mechanisms. We test our model on CartPoleSwingUpHarder [35], a more challenging variant where initial positions and velocities are highly randomized, increasing task variability. The agent observes the state vector  $[x, \dot{x}, \cos(\theta), \sin(\theta), \dot{\theta}]$  and outputs a scalar action at each timestep, receiving rewards for keeping  $x$  close to zero and  $\cos(\theta)$  close to one.

Formally, at each timestep  $t$ , the agent receives an observation  $o_t \in \mathbb{R}^5$ , defined as:

$$o_t = [x_t, \dot{x}_t, \cos(\theta_t), \sin(\theta_t), \dot{\theta}_t],$$

where  $x_t$  is the cart position,  $\dot{x}_t$  is the cart velocity,  $\theta_t$  is

the pole angle (represented using  $\cos$  and  $\sin$  to avoid discontinuities), and  $\dot{\theta}_t$  is the angular velocity. The policy network  $\pi(o_t, a_{t-1})$  takes the current observation and the previous action  $a_{t-1} \in \mathbb{R}$  as input and produces a scalar action  $a_t \in \mathbb{R}$ , which is applied as a continuous force to the cart. The objective is to maximize the cumulative reward, which increases as  $x_t \rightarrow 0$  and  $\cos(\theta_t) \rightarrow 1$ , indicating the cart is centered and the pole is upright.

This observation vector is then distributed across  $N = 5$  sensory neurons in the AttentionNeuron layer, where each neuron processes a single element of the observation, maintaining the permutation-invariant design.

Our policy network consists of two layers: an Attention-Neuron layer followed by a fully connected output layer. The AttentionNeuron layer is composed of  $N = 5$  sensory neurons, producing a latent representation  $m_t \in \mathbb{R}^{16}$ , which is then passed through a linear layer to output a scalar action. Both models (baseline and ours) are trained using CMA-ES, an evolutionary strategy optimization method.

To assess the impact of Nonlinear Attention (NLA), we modify the AttentionNeuron layer by applying a nonlinear transformation to the key vectors before computing self-attention as shown in equation 3. This transformation enhances feature expressivity by introducing quadratic interactions and a piecewise linear term, which improves gradient flow and learning dynamics. By incorporating NLA, the number of trainable parameters in the model increases slightly from 913 (baseline) to 998, reflecting the additional complexity introduced by the nonlinear mapping.

The two graphs illustrate the performance comparison between the baseline model and the Nonlinear Attention (NLA) model for the CartPole Swing-Up task. The first graph (Figure 2a) represents the convergence speed during training. The vertical axis shows the loss, where lower values indicate better optimization, and the horizontal axis represents the training steps. The NLA model (green) demonstrates significantly faster convergence compared to the baseline (red), reaching stability in fewer steps while maintaining a smoother optimization trajectory. The baseline, while improving initially, stabilizes at a higher loss, whereas the NLA model achieves a more stable and efficient learning process.

The second graph (Figure 2b) tracks the maximum fitness score achieved during training. The NLA model quickly attains a higher fitness score compared to the baseline, which gradually increases over time. This highlights that the NLA-enhanced model learns more efficiently, reaching optimal performance significantly earlier and demonstrating superior sample efficiency and generalization.

To further highlight the efficiency of our proposed ap-

Table 2: Comparison of both baseline and proposed model’s fitness scores after 5K iterations. Scores below shows fitness score and standard deviation over 1000 test episodes.

Model	Fitness Score
Baseline (Sensory Neuron)	265 $\pm$ 264
Proposed (NLA)	512 $\pm$ 419

proach, we compare the performance of both models at key convergence milestones. Table 2 summarizes the baseline model’s performance at the iteration where the NLA model converged. This clearly demonstrates that the NLA-enhanced model not only converges faster, but also achieves higher fitness and more stable optimization much earlier, validating its improved learning capacity and sample efficiency.

#### 4.2 PyBullet Ant

The PyBullet Ant (PyAnt) [36] task is a challenging reinforcement learning environment that involves controlling an eight-jointed quadruped to achieve stable locomotion. In this task, the agent receives an observation vector  $o_t \in \mathbb{R}^{28}$ , consisting of joint positions, joint velocities, and body orientation metrics from the quadruped’s eight limbs and torso. The action vector  $a_t \in \mathbb{R}^8$  specifies torque values applied to each of the eight joints. Formally, the policy  $\pi(o_t, a_{t-1})$  maps the current observation and previous action to a continuous action vector:

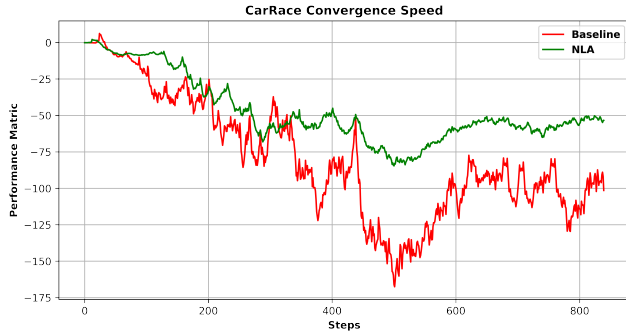
$$a_t = \pi(o_t, a_{t-1}) \in \mathbb{R}^8.$$

Each element  $o_t[i] \in \mathbb{R}^1$  of the observation is processed by one of the  $N = 8$  sensory neurons in the AttentionNeuron layer, ensuring consistent permutation-invariant processing across limbs. The objective is to maximize cumulative reward, which encourages forward movement while minimizing energy usage and maintaining balance.

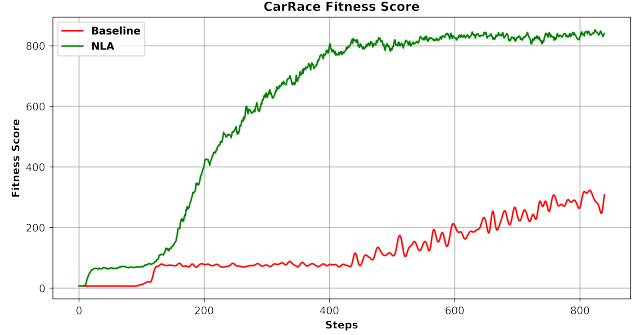
The high-dimensional observation and action spaces make this a suitable benchmark for evaluating the ability of the Nonlinear Attention mechanism to model inter-joint dependencies and promote stable locomotion.

Similarly to the CartPole setup, the policy network structure remains the same, with an AttentionNeuron layer (with Nonlinear transformation of key vectors) followed by a fully connected output layer. However, due to the increased input dimensionality  $N = 8$ , corresponding to the eight joints of the ant, the total number of trainable parameters differs. The baseline model has 2,504 parameters, while the NLA-enhanced model increases to 3,428 parameters, reflecting the additional complexity introduced by the nonlinear attention mechanism.

The two graphs compare the performance of the baseline model and the Nonlinear Attention (NLA) model on the Py-



(a) CarRace Convergence Speed



(b) CarRace Max Fitness Score

Figure 3: Comparison of convergence and performance in the CarRacing task: our NLA model not only learns faster (a), but also reaches a higher fitness score much earlier (b) than the baseline.

Bullet Ant (PyAnt) task, a more complex locomotion challenge requiring coordinated multi-joint control. Figure 2c shows the convergence speed, where the baseline (red) experiences a sharp performance drop mid-training before stabilizing, indicating instability in learning. In contrast, the NLA model (green) maintains a smoother and more stable descent, suggesting improved robustness in optimization.

Figure 2d presents the maximum fitness score, where the NLA model reaches a significantly higher performance level much earlier than the baseline. This demonstrates that NLA enables faster learning and better adaptation, crucial for complex tasks such as PyAnt that require efficient exploration and precise motor coordination.

Table 3: Comparison of both baseline and proposed model’s fitness scores after 5K iterations. Scores below shows fitness score and standard deviation over 100 test episodes.

Model	Fitness Score
Baseline (Sensory Neuron)	$327 \pm 35$
Proposed (NLA)	$2582 \pm 49$

Furthermore, Table 3 presents a direct comparison of fitness scores between the two models. It highlights the baseline model’s performance at the iteration where the NLA model has already converged. The NLA-enhanced agent achieves the same level of performance with significantly fewer iterations, demonstrating improved learning efficiency and faster adaptation in high-dimensional, multi-joint control tasks compared to the baseline Sensory Neuron model.

### 4.3 CarRacing

To evaluate the effectiveness of our proposed Nonlinear Attention (NLA) mechanism, we conduct experiments on the CarRacing environment [37], following the same setup as in the baseline Sensory Neuron model [8]. Our focus is on analyzing both convergence speed and out-of-domain gen-

eralization in a visually complex control task.

In this task, the agent receives an observation  $o_t \in \mathbb{R}^{96 \times 96 \times 4}$ , consisting of four stacked grayscale frames from the environment. This high-dimensional visual input is split into  $N = 256$  non-overlapping patches of size  $6 \times 6 \times 4$ , resulting in local sensory inputs  $o_t[i] \in \mathbb{R}^{144}$  for each sensory neuron. The AttentionNeuron layer processes each patch independently to compute key and value vectors, while the query is generated from a fixed set of  $M = 1024$  learned seed embeddings.

Formally, the output of the attention mechanism is a latent representation  $m_t \in \mathbb{R}^{1024 \times d}$ , where  $d$  is the embedding dimension. This output is reshaped into a spatial map  $m_t \in \mathbb{R}^{32 \times 32 \times 16}$  and passed to a downstream Attention-Agent policy network that applies hard attention to select relevant features. The reward function encourages smooth driving and track adherence, with higher scores achieved by maintaining speed while minimizing off-track penalties.

The introduction of Nonlinear Attention enhances the key representations before attention computation, allowing for richer interactions between the input patches and the learned queries. This added expressiveness enables the agent to more effectively distinguish between relevant and redundant visual features, which accelerates convergence and improves generalization.

We begin by comparing our model to the baseline architecture, which uses a permutation-invariant AttentionNeuron layer to process a shuffled set of input patches. The output is reshaped to a latent tensor  $m_t \in \mathbb{R}^{32 \times 32 \times 16}$ , which is then passed to an AttentionAgent policy network [27] that applies hard attention to select the most relevant features. The full system is trained using Evolution Strategies (ES), as the hard attention mechanism is non-differentiable.

Our model retains this architecture but introduces a nonlin-

ear Attention transformation applied to the key vectors before the attention computation as shown in equation 3. This modification enhances the expressiveness of the attention mechanism by introducing quadratic and piecewise-linear relationships between the query and key vectors. Importantly, it maintains the permutation-invariant property of the original AttentionNeuron design.

As shown in Figure 3a and Figure 3b, our model not only converges significantly faster than the baseline, but also achieves maximum fitness scores, which can be seen from Table 4. Although the baseline requires approximately 3,000 iterations to reach stable performance, our model achieves comparable results in under 800 iterations. This improvement is evident in the training curves, which show a sharper increase in fitness and earlier plateauing, indicating better sample efficiency and faster learning.

Table 4: Comparison of both baseline and proposed model’s fitness scores after 800 iterations. Scores below shows fitness score and standard deviation over 100 test episodes.

Model	Fitness Score
Baseline (Sensory Neuron)	383 ± 184
Proposed (NLA)	827 ± 34

Overall, these findings confirm that NLA significantly improves convergence speed and robustness in visually complex reinforcement learning environments, while retaining the core advantages of permutation invariance.

#### 4.4 Atari Pong

The last environment where we evaluated NLA is the Atari Pong environment [38], under a challenging screen-shuffled setting. Each observation frame is divided into non-overlapping patches, which are shuffled before being passed to the agent. The goal is to determine whether NLA can help the agent reconstruct spatial structure and learn robust policies from unordered visual inputs.

In the Atari Pong setup, the agent receives grayscale observations  $o_t \in \mathbb{R}^{84 \times 84 \times 4}$ , composed of four stacked frames. These frames are partitioned into  $N = 196$  non-overlapping patches of size  $6 \times 6 \times 4$ , with each local patch represented as  $o_t[i] \in \mathbb{R}^{144}$ . The permutation-invariant AttentionNeuron layer processes these unordered patches to produce a latent message  $m_t \in \mathbb{R}^{400 \times 32}$ , where the fixed query set has  $M = 400$  learned embeddings.

This latent code is reshaped into a structured spatial format  $m_t \in \mathbb{R}^{20 \times 20 \times 32}$ , which serves as the input to a downstream convolutional neural network (CNN). The CNN maps the representation to logits over six discrete actions  $a_t \in \{0, 1, \dots, 5\}$ , using the architecture described in the main text. The behavior cloning objective minimizes the

mean squared error between the student’s logits  $\hat{a}_t$  and those of a teacher policy  $a_t^{\text{teacher}}$ , i.e.,

$$\mathcal{L}_{\text{BC}} = \frac{1}{B} \sum_{i=1}^B \|\hat{a}_t^{(i)} - a_t^{\text{teacher}(i)}\|^2,$$

where  $B$  is the batch size.

By learning from unordered inputs and reconstructing structured latent representations, the NLA-enhanced model improves learning efficiency and generalization under challenging visual conditions.

Our architecture builds on the baseline AttentionNeuron layer, but replaces its standard attention with the NLA transformation (equation 3). The resulting latent message  $m_t \in \mathbb{R}^{400 \times 32}$  is reshaped to a 2D format  $m_t \in \mathbb{R}^{20 \times 20 \times 32}$ , allowing us to append a deep convolutional neural network (CNN) that benefits from the restored spatial layout. The CNN architecture is as follows: [Conv(in=32, out=64, kernel=4, stride=2), Conv(in=64, out=64, kernel=3, stride=1), FC(in=3136, out=512), FC(in=512, out=6)]. We use ReLU activations in all layers. The final output represents logits over six discrete actions.

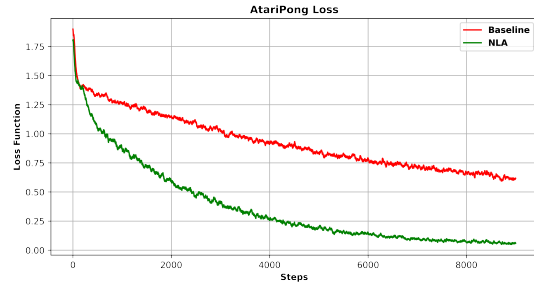


Figure 4: Convergence curve (MSE loss): the NLA-based agent minimizes the BC training loss much faster than the baseline, converging within 9K iterations.

To train the model, we adopt a behavior cloning (BC) approach. A teacher policy, trained via PPO, generates 1,000 rollouts from which we collect stacked observation patches and their corresponding action logits. The student policy is trained using mean squared error (MSE) loss to regress the teacher’s logits. We used a batch size of 256, and kept the learning rate and gradient norm clipping identical to previous experiments.

As shown in Figure 4, our model converges in less than 9K iterations, significantly faster than the 90K iterations required by the baseline model. Evaluation results are presented in Table 5, confirming that the NLA-based agent performs comparably or better under the same testing setup.

**Training Setup and Resource Usage** All experiments were conducted on a high-performance workstation equipped

Table 5: Comparison of both baseline and proposed model’s evaluation score after 9K iterations. Scores below shows fitness score and standard deviation over 100 test episodes. All environments except for Atari Pong have a hard limit of 1000 time steps per episode. In Atari Pong, while the maximum length of an episode does not exist, we observed that an episode usually lasts for around 2500 time steps.

Model	Evaluation Score
Baseline (Sensory Neuron)	$-21 \pm 2$
Proposed (NLA)	$21 \pm 0$

with an AMD Ryzen ThreadRipper Pro 5945WX (12 cores / 24 threads), an NVIDIA RTX A6000 GPU, and 64GB of RAM. Training was performed using PyTorch, and optimization was carried out using either behavior cloning (BC) for AtariPong and evolution strategies (ES) for the rest of the environments. Each model was trained individually per environment without parallelization or distributed training.

Table 6: Comparison of Convergence Iterations and Training Time (in days) for both baseline and proposed models.

Environment	Baseline		Proposed (NLA)	
	Iterations	Time	Iterations	Time
CartPole Swing-Up	14K	6	5K	2
PyBullet Ant (PyAnt)	15K	36	5K	9
CarRace	4K	73	700	25
Atari Pong (BC)	90K	16	9K	2

Table 6 provides a comparison of the number of iterations and wall-clock time required for convergence across all four environments. It clearly shows that the proposed NLA-enhanced model consistently achieves convergence faster—both in terms of iterations and time—compared to the baseline Sensory Neuron model. This efficiency highlights the practical benefits of incorporating nonlinear attention, especially when computational resources or training budgets are limited.

**5. Discussion Applications:** The introduction of Nonlinear Attention (NLA) offers a key advantage in terms of representational complexity and expressivity. By applying nonlinear transformations to the key vectors, the model captures higher-order feature interactions that are otherwise inaccessible through standard linear attention. This enriched representation enables agents to more rapidly identify task-relevant patterns within unordered or noisy inputs, facilitating faster convergence and more effective learning. In practical applications, such refined latent spaces may strengthen the underlying permutation-invariant property by allowing the agent to internally reconstruct coherent structures from disordered inputs, making NLA particularly valuable in settings where observation order is unreliable or dynamically

changing, such as in sensor fusion, modular robotics, or adaptive control systems.

**Limitations:** While NLA improves learning efficiency, several limitations remain. First, the expressivity gains come at the cost of slightly increased parameter count and computation. Although the overhead is minimal compared to the performance gains, large-scale deployments must still consider this trade-off. Second, in visual environments, the choice of patch size continues to influence both computational cost and model performance. We find that moderate patch sizes (e.g.,  $6 \times 6$ ) strike a balance between context representation and attention matrix scalability. Extremely small patches, such as  $1 \times 1$  pixels, significantly degrade performance and inflate computation due to large attention matrices.

Additionally, like its baseline counterpart, our architecture only applies permutation invariance to the input side. Outputs, such as action vectors, remain sensitive to ordering. Extending permutation invariance to outputs would require modeling actions as independent, self-attending modules — a direction we leave for future exploration.

**Societal Impact:** One of the central contributions of this work is its emphasis on computational efficiency, which we believe has meaningful societal implications. The NLA model enables agents to learn complex tasks using significantly fewer iterations and in less time than baseline approaches. This efficiency allows researchers, developers, and students with limited computational access to experiment with attention-based models and reinforcement learning without requiring large-scale infrastructure.

Instead of waiting weeks or months for model convergence, agents equipped with NLA can often be trained in a matter of days, while achieving competitive performance. This improved accessibility promotes more equitable participation in machine learning research and lowers the environmental cost associated with training compute-heavy models. However, as with any powerful optimization tool, responsible deployment remains critical. Potential applications of attention-based policies span robotics, surveillance, and real-time analytics. Care should be taken to ensure that such systems are used transparently and ethically, especially when operating on human-centric data or in decision-critical environments.

**Future Work:** A promising future direction is to extend the permutation invariance property to the action layer. One possibility is to model each motor output as a separate “motor neuron” connected via attention to latent representations, allowing for flexible, modular action control. Such a framework could enable general-purpose policies capable of adapting to different morphologies — e.g., agents with varying numbers of limbs or dynamic joint configurations

— simply by reconfiguring attention links.

Another direction could be to focus on making NLA lighter and faster, without losing its ability to learn rich features — so it could be used in real-world robots or low-power devices. Also, by connecting attention mechanisms to the reward signal, we could help agents automatically figure out which parts of their input are useful for decision-making, leading to more adaptive and intelligent behavior.

**7. Acknowledgments** I would like to thank Ahsan Adeel for his guidance in the initial stages of this work. I am also grateful to Ingo Fromholz and Zeeshan Parzeez for their valuable insights and continued supervision. Special thanks to Khubaib Ahmed and Ahsan ul Haq for their consistent support during the course of this research.

## References

- [1] Y. Tang and D. Ha, “The sensory neuron as a transformer: Permutation-invariant neural networks for reinforcement learning,” in *Thirty-Fifth Conference on Neural Information Processing Systems*, 2021.
- [2] J. Ba, G. Hinton, V. Mnih, J. Z. Leibo, and C. Ionescu, “Using fast weights to attend to the recent past,” *arXiv preprint arXiv:1610.06258*, 2016.
- [3] D. Ha, A. Dai, and Q. V. Le, “Hypernetworks,” *arXiv preprint arXiv:1609.09106*, 2016.
- [4] J. Schmidhuber, “Learning to control fast-weight memories: An alternative to dynamic recurrent networks,” *Neural Computation*, vol. 4, no. 1, pp. 131–139, 1992.
- [5] T. Miconi, A. Rawal, J. Clune, and K. O. Stanley, “Backpropamine: Training self-modifying neural networks with differentiable neuromodulated plasticity,” 2020.
- [6] T. Miconi, K. Stanley, and J. Clune, “Differentiable plasticity: Training plastic neural networks with back-propagation,” in *Proceedings of the 35th International Conference on Machine Learning (ICML)*. PMLR, 2018, pp. 3559–3568.
- [7] E. Najarro and S. Risi, “Meta-learning through hebbian plasticity in random networks,” *arXiv preprint arXiv:2007.02686*, 2020.
- [8] B. Amos, I. D. J. Rodriguez, J. Sacks, B. Boots, and J. Z. Kolter, “Differentiable mpc for end-to-end planning and control,” *arXiv preprint arXiv:1810.13400*, 2018.
- [9] M. P. Deisenroth and C. E. Rasmussen, “Pilco: a model-based and data-efficient approach to policy search,” in *Proceedings of the 28th International Conference on Machine Learning*, 2011, p. 465–472.
- [10] D. Ha and J. Schmidhuber, “Recurrent world models facilitate policy evolution,” in *Advances in Neural Information Processing Systems*, vol. 31, 2018.
- [11] D. Hafner, T. Lillicrap, I. Fischer, R. Villegas, D. Ha, H. Lee, and J. Davidson, “Learning latent dynamics for planning from pixels,” *arXiv preprint arXiv:1811.04551*, 2018.
- [12] J. Lee, Y. Lee, J. Kim, A. Kosiorek, S. Choi, and Y. W. Teh, “Set transformer: A framework for attention-based permutation-invariant neural networks,” in *Proceedings of the 36th International Conference on Machine Learning*, ser. Proceedings of Machine Learning Research, vol. 97. PMLR, 2019, pp. 3744–3753.
- [13] A. Vaswani, N. Shazeer, N. Parmar, J. Uszkoreit, L. Jones, A. N. Gomez, Ł. Kaiser, and I. Polosukhin, “Attention is all you need,” *Advances in neural information processing systems*, vol. 30, 2017.
- [14] J. Schmidhuber, “Reducing the ratio between learning complexity and number of time varying variables in fully recurrent nets,” in *International Conference on Artificial Neural Networks*. Springer, 1993, pp. 460–463.
- [15] A. Graves, G. Wayne, and I. Danihelka, “Neural Turing machines,” *arXiv preprint arXiv:1410.5401*, 2014.
- [16] M.-T. Luong, H. Pham, and C. D. Manning, “Effective approaches to attention-based neural machine translation,” *arXiv preprint arXiv:1508.04025*, 2015.
- [17] T. B. Brown, B. Mann, N. Ryder, M. Subbiah, J. Kaplan, P. Dhariwal, A. Neelakantan, P. Shyam, G. Sastry, A. Askell *et al.*, “Language models are few-shot learners,” *arXiv preprint arXiv:2005.14165*, 2020.
- [18] J. Devlin, M. Chang, K. Lee, and K. Toutanova, “BERT: pre-training of deep bidirectional transformers for language understanding,” 2018.
- [19] A. Dosovitskiy, L. Beyer, A. Kolesnikov, D. Weissenborn, X. Zhai, T. Unterthiner, M. Dehghani, M. Minderer, G. Heigold, S. Gelly, J. Uszkoreit, and N. Houlsby, “An image is worth 16x16 words: Transformers for image recognition at scale,” in *International Conference on Learning Representations (ICLR)*, 2021.

- [20] P. Esser, R. Rombach, and B. Ommer, “Taming transformers for high-resolution image synthesis,” *arXiv preprint arXiv:2012.09841*, 2020.
- [21] R. Girdhar, J. Carreira, C. Doersch, and A. Zisserman, “Video action transformer network,” in *Proceedings of the IEEE/CVF Conference on Computer Vision and Pattern Recognition (CVPR)*, 2019, pp. 244–253.
- [22] A. Jaegle, F. Gimeno, A. Brock, A. Zisserman, O. Vinyals, and J. Carreira, “Perceiver: General perception with iterative attention,” *arXiv preprint arXiv:2103.03206*, 2021.
- [23] C. Sun, F. Baradel, K. Murphy, and C. Schmid, “Contrastive bidirectional transformer for temporal representation learning,” 2019.
- [24] J. Choi, B.-J. Lee, and B.-T. Zhang, “Multi-focus attention network for efficient deep reinforcement learning,” *arXiv preprint arXiv:1712.04603*, 2017.
- [25] A. Mott, D. Zoran, M. Chrzanowski, D. Wierstra, and D. J. Rezende, “Towards interpretable reinforcement learning using attention augmented agents,” *arXiv preprint arXiv:1906.02500*, 2019.
- [26] I. Sorokin, A. Seleznev, M. Pavlov, A. Fedorov, and A. Ignateva, “Deep attention recurrent q-network,” *arXiv preprint arXiv:1512.01693*, 2015.
- [27] Y. Tang, D. Nguyen, and D. Ha, “Neuroevolution of self-interpretable agents,” in *Proceedings of the Genetic and Evolutionary Computation Conference (GECCO)*, 2020. [Online]. Available: <https://attentionagent.github.io>
- [28] V. Zambaldi, D. Raposo, A. Santoro, V. Bapst, Y. Li, I. Babuschkin, K. Tuyls, D. Reichert, T. Lillicrap, E. Lockhart, M. Shanahan, V. Langston, R. Pascanu, M. Botvinick, O. Vinyals, and P. Battaglia, “Deep reinforcement learning with relational inductive biases,” in *International Conference on Learning Representations (ICLR)*, 2019.
- [29] K. Lee, K. Lee, J. Shin, and H. Lee, “Network randomization: A simple technique for generalization in deep reinforcement learning,” in *International Conference on Learning Representations (ICLR)*, 2020.
- [30] S. Hochreiter and J. Schmidhuber, “Long short-term memory,” *Neural Computation*, vol. 9, no. 8, pp. 1735–1780, 1997.
- [31] J. L. Ba, J. R. Kiros, and G. E. Hinton, “Layer normalization,” *arXiv preprint arXiv:1607.06450*, 2016. [Online]. Available: <https://arxiv.org/abs/1607.06450>
- [32] A. Gaier and D. Ha, “Weight agnostic neural networks,” in *Advances in Neural Information Processing Systems*, 2019. [Online]. Available: <https://arxiv.org/abs/1906.04358>
- [33] Y. Gal, R. McAllister, and C. E. Rasmussen, “Improving pilco with bayesian neural network dynamics models,” in *Data-Efficient Machine Learning workshop, ICML*, 2016. [Online]. Available: <https://arxiv.org/abs/1505.05324>
- [34] Anonymous, “Pytorch implementation of improving pilco with bayesian neural network dynamics models,” 2023. [Online]. Available: <https://github.com/yourusername/pytorch-pilco>
- [35] C. D. Freeman, L. Metz, and D. Ha, “Learning to predict without looking ahead: World models without forward prediction,” in *Advances in Neural Information Processing Systems*, 2019. [Online]. Available: <https://arxiv.org/abs/1910.13038>
- [36] E. Coumans and Y. Bai, “Pybullet, a python module for physics simulation for games, robotics and machine learning,” <http://pybullet.org>, 2016–2021.
- [37] O. Klimov, “Carracing,” URL <https://gym.openai.com/envs/CarRacing-v0>, 2016.
- [38] G. Brockman, V. Cheung, L. Pettersson, J. Schneider, J. Schulman, J. Tang, and W. Zaremba, “Openai gym,” *arXiv preprint arXiv:1606.01540*, 2016.